

# Experiments in Ultrasonic Flaw Detection using a MEMS Transducer

Akash Jain<sup>a</sup>, David W. Greve<sup>a</sup>, Irving J. Oppenheim<sup>b\*</sup>

<sup>a</sup>Department of Electrical and Computer Engineering

<sup>b</sup>Department of Civil and Environmental Engineering, Carnegie Mellon University

## ABSTRACT

In earlier work we developed a MEMS phased array transducer, fabricated in the MUMPs process, and we reported on initial experimental studies in which the device was affixed into contact with solids. We demonstrated the successful detection of signals from a conventional ultrasonic source, and the successful localization of the source in an off-axis geometry using phased array signal processing. We now describe the predicted transmission and coupling characteristics for such devices in contact with solids, demonstrating reasonable agreement with experimental behavior. We then describe the results of experiments attempting to discriminate between direct signal incidence and reflection from a flaw in a specimen, as well as results for fluid-coupled detectors.

**Keywords :** Ultrasonics, MEMS, phased array, diaphragm, capacitive transducer

## 1. INTRODUCTION

Ultrasonic pulse-echo detection is used in flaw detection<sup>1</sup> and in many other applications such as range/motion sensing, embedded object detection, surface characterization, and medical ultrasound imaging. Commercial transducers typically use piezoceramics such as PZT (lead-zirconium-titanate) but our research is directed at the development of MEMS phased array transducers to be installed as resident devices to monitor critical locations on steel structures. Microscale ultrasonic diaphragm design has been studied for application to air-coupled and fluid-coupled applications, and is covered comprehensively in articles by Khuri-Yakub<sup>2,3,4,5,6</sup>. One paper<sup>2</sup> outlines the mechanical and electrical analysis of capacitive diaphragm transducers and presents experimental results for air-coupled and fluid-coupled transmission through aluminum, showing the feasibility of applications including flaw detection. A second paper<sup>3</sup> records the fabrication steps needed to produce capacitive ultrasonic transducers suitable for immersion applications and the characterization, both experimental and analytical, of their performance. Another<sup>4</sup> presents results for nondestructive evaluation of metal specimens, in which air-coupled transducers generate and receive Lamb waves, which are useful for detecting near-surface flaws. Two other references<sup>5,6</sup> discuss one-dimensional transducer arrays and present initial imaging results, in which solids immersed within fluids are detected. Other investigators of MEMS ultrasonics include Schindel<sup>7,8</sup> with numerous contributions to immersion applications, and Eccardt<sup>9,10</sup>, with the demonstration of surface micromachined transducers in a modified CMOS process.

We developed a MEMS transducer and have studied its use in direct contact with solids. We first presented the work at this SPIE conference<sup>11</sup> in 2002, and reported additional results in subsequent papers<sup>12,13,14</sup>, in one article<sup>15</sup> on device characterization, and in a second article<sup>16</sup> on transmission when coupled directly to a solid. In this paper we briefly summarize those findings and present further experimental results relating to flaw detection and to transducer performance when fluid-coupled.

## 2. TECHNICAL APPROACH

MEMS capacitive (diaphragm-type) transducers are not effective at transmitting energy into a solid because the energy that can be developed in such a structure is small. In our experiments a commercial ultrasonic PZT transducer acts as the excitation source and the MEMS transducers on our chip operate as receivers in a phased-array geometry. In a

---

\* Contact author: ijo@cmu.edu; 412-268-2950; Carnegie Mellon University, Department of Civil and Environmental Engineering, Pittsburgh, PA 15213.

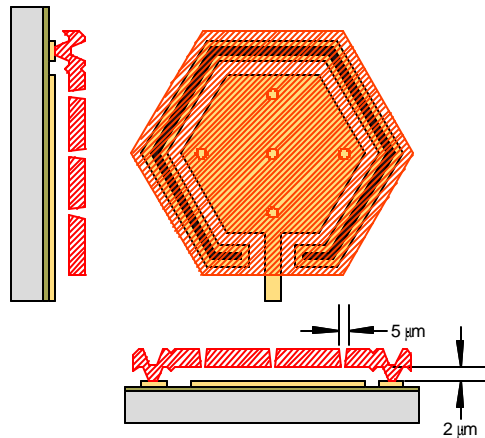


Figure 1. Layout and cross-section showing typical poly-1 hexagonal diaphragms; 180 diaphragms per transducer

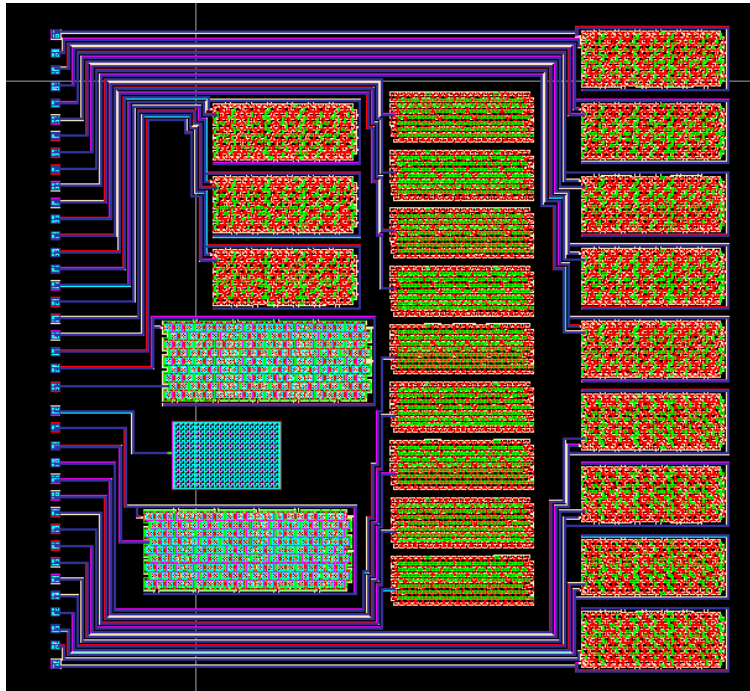


Figure 2. Layout of MEMS device, approximately 1 cm square, array of nine transducers in column at right

capacitive (diaphragm-type) transducer, diaphragm deflection produces a change in capacitance which can be detected electrically when a DC bias voltage is maintained across the plates of the capacitor. The sensitivity of any single diaphragm increases linearly with the bias voltage and inversely with the square of the original (undeflected) gap dimension, and the sensitivity of any transducer composed of diaphragms in parallel increases with the number of diaphragms. The device was designed for fabrication by the MUMPS surface micromachining process, and Figure 1 is a sketch of a typical hexagonal diaphragm. It is constructed in the polysilicon-1 structural layer, with a thickness of  $2\ \mu\text{m}$ , and the holes are required per MUMPS design rules for the release etch of the sacrificial layer between the poly-1 layer and the substrate. The diaphragm geometry is a regular hexagon and the length of each leg is equal to  $49\ \mu\text{m}$ , with a

measured resonant frequency near 3.5 MHz. The underlying electrode area is hexagonal with leg length equal to 37.5  $\mu\text{m}$ , and the gap between the diaphragm and the electrode area on the substrate is 2  $\mu\text{m}$ , from which the predicted capacitance for a single diaphragm is 0.016 pf. A target capacitance of a few pf is required, and we designed our basic transducer to contain 180 diaphragms in parallel for a predicted capacitance of 2.9 pf; the transducer is approximately 0.9 mm wide and 2 mm long. The layout drawing for the overall chip, approximately 1 cm square, is shown in Figure 2. The column of nine transducers at the east is the primary array, the column just east of center is an array of nine transducers using an alternate diaphragm design, and the column just west of center is a group of structures prepared for additional physics experiments; all results presented in this paper are obtained from the primary array at the east.

### 3. DISCUSSION OF ACOUSTIC COUPLING

In our experiments the MEMS device was bonded to plexiglass specimens using Gelest Zipcone CG silicone adhesive. The thickness of the adhesive layer, denoted as  $t$  and measured to be approximately 20  $\mu\text{m}$ , is small compared to the acoustic wavelength of that silicone, denoted as  $\lambda$  and calculated at 3.5 MHz to be 370  $\mu\text{m}$ . Figure 3 is a transmission line model<sup>14,16</sup> showing the solid specimen with acoustic impedance  $Z_m$ , the silicone layer with acoustic impedance  $Z_{\text{silicone}}$ , and the diaphragm transducer with acoustic impedance  $Z_{\text{transducer}}$ .

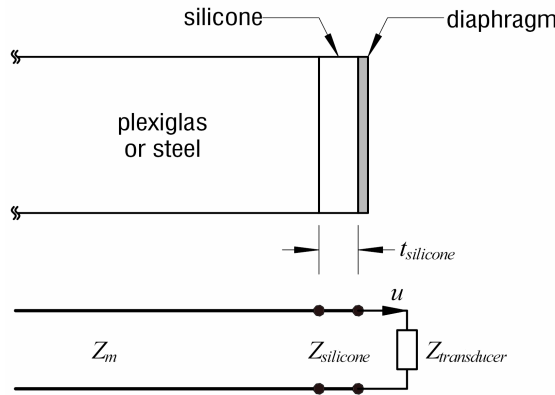


Figure 3. Transmission line model showing a solid specimen, a silicone coupling layer, and a diaphragm transducer

We seek to compare the diaphragm velocity to the velocity that an incident ultrasonic wave would produce at the free surface of the solid medium, and we define that ratio as the gain  $G$ . Recognizing that  $Z_{\text{transducer}}$  is small compared to  $Z_{\text{silicone}}$  and can therefore be set to zero, the transmission line model yields:

$$G = \left\{ 1 + \left[ \frac{Z_{\text{silicone}}^2}{Z_m^2} - 1 \right] \sin^2 \left( \frac{2\pi t}{\lambda} \right) \right\}$$

Because  $t$  is considerably less than  $\lambda$ , we predict  $G$  to be close to 1 and relatively constant, regardless of the ratio of  $Z_{\text{silicone}}$  to  $Z_m$ . Use of air as a coupling medium would be less desirable because  $t$  would typically be some multiples of  $\lambda$  and  $G$  would be small when compared to 1. Moreover, the diaphragm transducer is heavily damped by the silicone adhesive, which is necessary for pulse-echo flaw detection because we require good pulse response. In contrast, the use of air as a coupling medium makes it difficult to achieve such response. In characterization experiments<sup>15</sup> we measured a  $Q$  of 49.6 at atmospheric pressure; in such a case vibration would cause the diaphragm to ring, making it ineffective at detecting distinct pulses. We will discuss this point in section 5 of this paper, where we examine experimental results of flaw detection from reflected signals.

#### 4. DETECTION OF ULTRASONIC SIGNALS AND PHASED ARRAY PERFORMANCE

A Krautkramer MSW-QV ultrasonic transducer with a rated operating frequency of 3.5 MHz, driven by a Krautkramer USPC-2100, was the signal source. The PZT transducer has a nominal diameter of 15 mm and produces a high-energy planar wave. The MEMS diaphragm transducers were biased with 100 V DC and the detected signal was averaged and recorded using a HP-54601A oscilloscope. Figure 4 depicts the plexiglass test specimen illuminating the transducer array at an extreme raking angle,  $65^\circ$  away from normal incidence at a center-to-center distance of 2.3 cm.

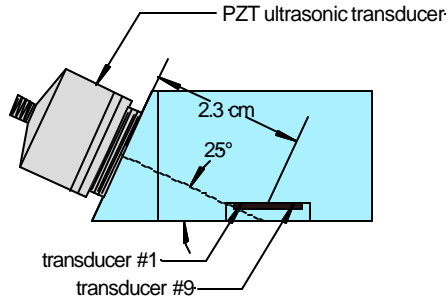


Figure 4. Sketch of specimen for off-axis (raking) geometry

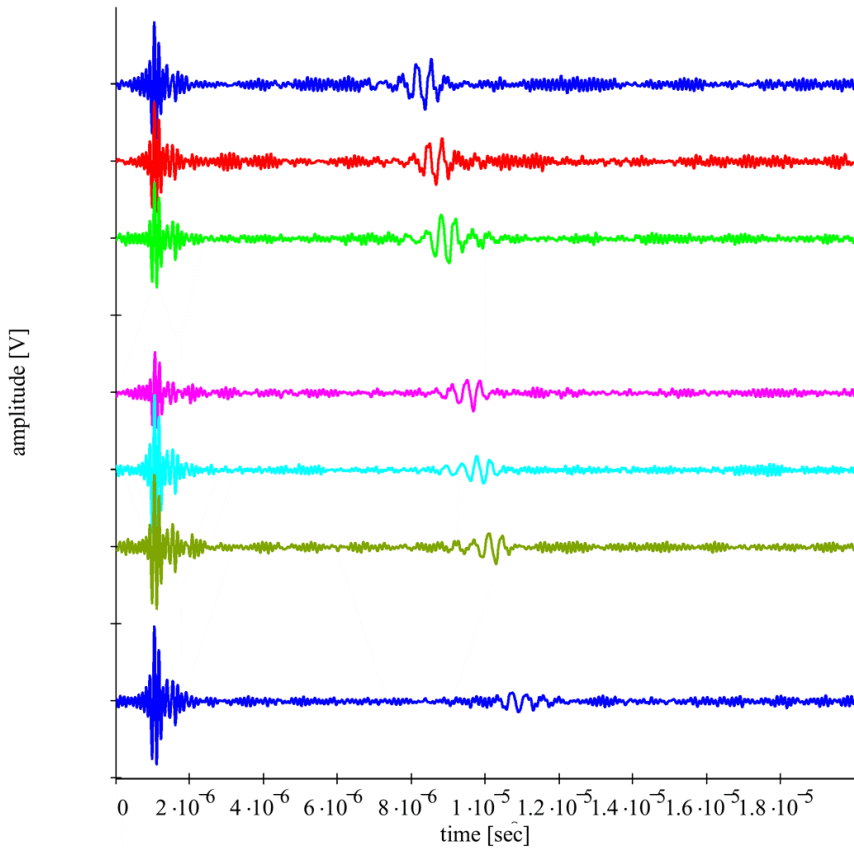


Figure 5. Experimental results, MEMS phased array response, off-axis incidence

Figure 5 displays the signals measured at seven transducers within the array; transducers #4 and #7 had failed during the course of the experiments. The seven signals are plotted on Figure 5 in their relative position within the array. Stray electrical coupling produces the signal observed uniformly at roughly  $1 \mu\text{s}$ , conveniently marking the start of the pulse. The signal arrival time at the center of the array, transducer #5, is approximately  $8.7 \mu\text{s}$ , and varies linearly along the

array, equivalent to a delay between adjacent transducers of 330 ns. Using those two measured quantities, with a speed of sound in plexiglass of 2700 m/s, we calculate a center-to-center distance of 2.35 cm and an incidence angle of  $61^\circ$  from the normal. These results compare favorably to the specimen dimensions recorded in Figure 4. The calculation was made using a collocation method<sup>14,16</sup> in which the signals were shifted and added, with the best estimate of center-to-center distance and incidence angle identified by a peak as shown in Figure 6.

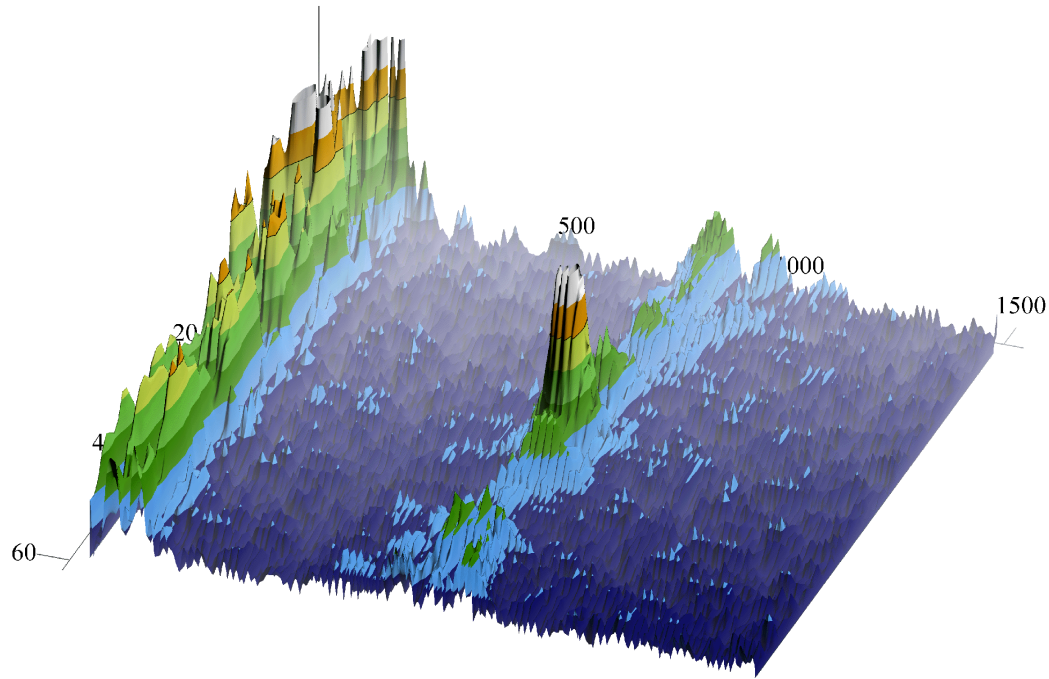


Figure 6. Collocation method of signal processing obtaining center-to-center distance and incidence angle

## 5. FLAW DETECTION FROM A REFLECTED WAVE

Figure 7, a sketch, depicts the elevation view of a plexiglass specimen where the MEMS device is positioned to receive a reflected wave<sup>14</sup>. The array of transducers is placed transverse to the direction of wave travel, meaning that negligible phase delay should be present in this experiment. Two “flaws” were induced in the wave path by drilling flat-bottomed holes, with the intention of detecting reflections from those bottom planes. The coarser hole has a diameter of 10 mm and the finer hole has a diameter of 4 mm, and the two bottom planes are separated from one another by 7.4 mm; at the frequency of 3.5 MHz an ultrasonic wave in plexiglass has an acoustic wavelength near 0.8 mm.

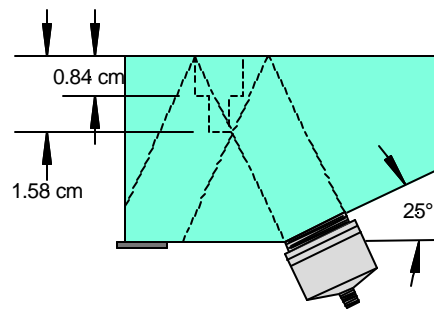


Figure 7. Specimen containing two flaws, for detection of signal reflected from flaw surfaces

Figure 8 displays the signals received across the array of nine transducers, using a preamplifier with a gain of 11. At each transducer three reflections are detected: from the fine flaw, arriving at 20.9  $\mu\text{s}$ , from the coarse flaw, arriving at 24.1  $\mu\text{s}$ , and from the back surface of the specimen, arriving at 29.3  $\mu\text{s}$ . These results are in good agreement with values of 18.6, 23.7, and 29.6  $\mu\text{s}$ , respectively, calculated from the specimen dimensions. The reflection off the fine flaw is detectable, and is distinguishable from the reflection off the coarse flaw only 7.4 mm away.

The need for high damping to obtain good pulse response can be appreciated when examining the signals in Figure 8. If the signals were placed in reverse order, the small signal from the fine flaw could be detected following the strongest signal if the peaks were separated by perhaps 2  $\mu\text{s}$ , a time interval that corresponds to 7 cycles at 3.5 MHz. However, if the transducer had a mechanical Q of 49.6, as measured<sup>15</sup> in air, after 7 cycles the first signal would still be at 64% of its peak amplitude, and this “ringing” that would prevent the detection of another peak for some long interval.

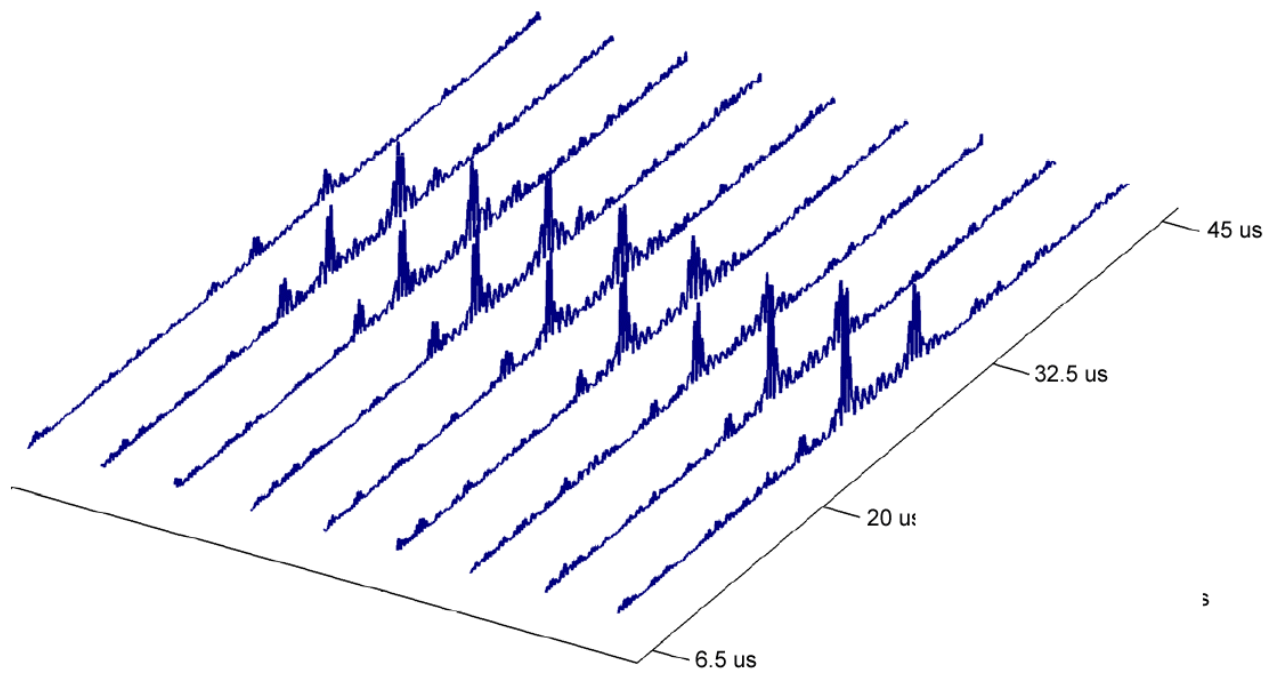


Figure 8. Signals received across transducer array from fine flaw, from coarse flaw, and from back surface

## 6. DEMONSTRATION OF FLUID-COUPLED PERFORMANCE

One device was wire bonded in an open ceramic package and embedded under a layer of silicone adhesive with an approximate thickness of 1.5 mm. The silicone layer served as a level base and seal for a cylindrical tank holding a volume of water. Figure 9 is a sectional sketch depicting the package, the MEMS device, and the silicone layer, showing a 5 MHz Krautkramer PZT transducer in two positions at which experiments were conducted, 15 mm (“large gap”) and 5 mm from the base; the tank walls and the water are not shown in Figure 9. Figure 10 shows the 1 MHz C(V) characteristics before and after application of the silicone. The characteristic hysteresis of a silicone-bonded transducer is detected.

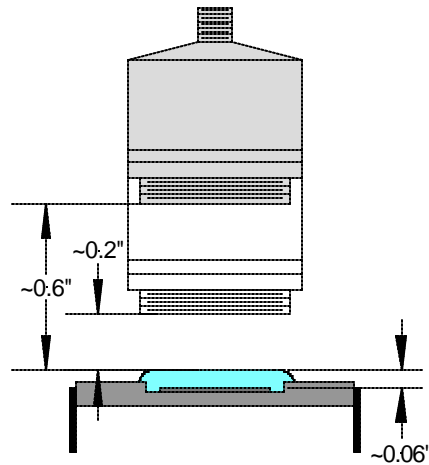


Figure 9. Cross-section of fluid coupled experiment showing ceramic package, MEMS device, silicone, and PZT positions

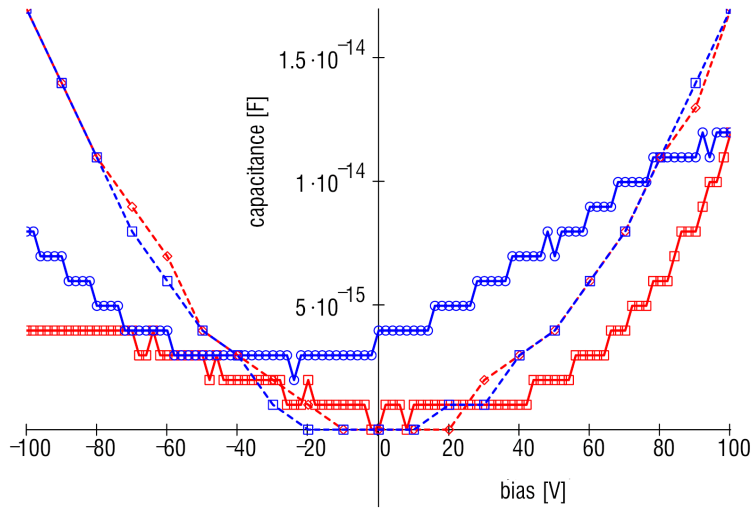


Figure 10. Measured 1 MHz C(V) characteristics before and after application of silicone

The upper plot in Figure 11 shows the signal detected by the MEMS transducer (with a bias voltage of 100 V DC) in response to the Krautkramer transducer in the “large gap” position, with the Krautkramer transducer signal on the lower plot. Again, stray electrical coupling provides a convenient trigger mark at the start of the MEMS record. The delay between the trigger and the received pulse is approximately 10  $\mu\text{s}$ , roughly corresponding to the time interval needed for the wave to travel through the 15 mm depth of water and the 1.5 mm thickness of silicone. The second signal observed by the MEMS transducer, delayed by an additional 2.9  $\mu\text{s}$ , is in fair agreement with the delay expected for a signal reflected from the MEMS chip, reflected again at the silicone-water interface, and then observed again by the MEMS transducer.

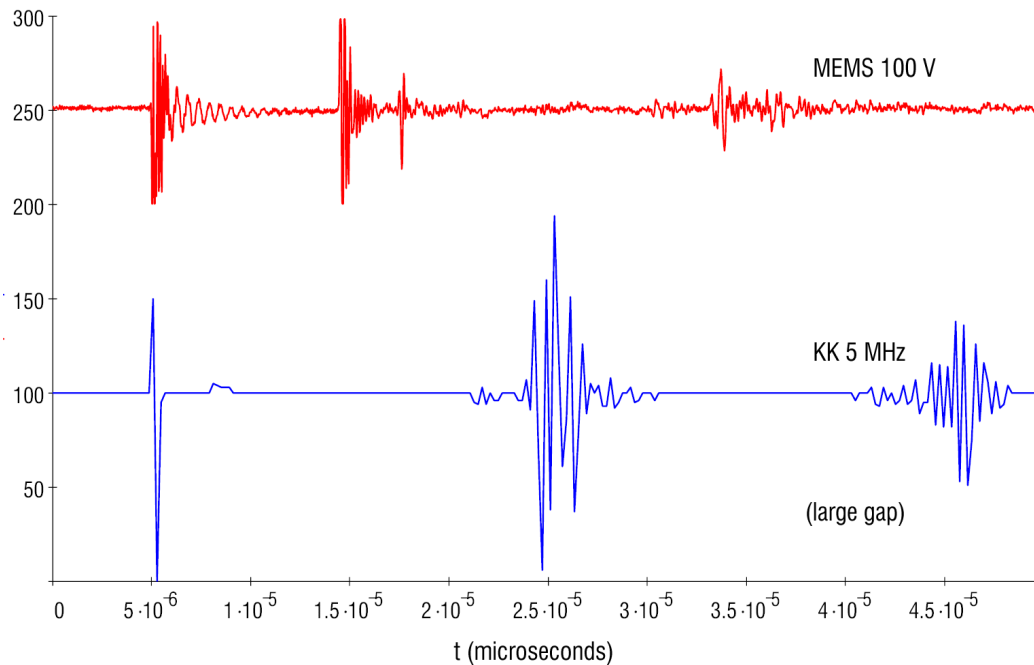


Figure 11. Observed signals, fluid coupled experiment, large (15 mm) gap

## 7. CONCLUSIONS

Experimental results in Figures 5 and 6 show that MEMS transducers can successfully detect ultrasonic pulses when fixed into contact with solids and that a phased array implementation can successfully localize sources from off-axis geometries. Experimental results in Figures 7 and 8 show that MEMS transducers, fixed into contact with solids, can detect reflections from relatively small flaws and have good pulse response, providing good resolution of flaw geometry. Experimental results in Figures 9 through 11 show that MEMS transducers can be sealed with a silicone layer and operate through fluid coupling.

The acoustic coupling of a MEMS capacitive (diaphragm-type) transducer to a solid, through a silicone layer, has been analysed using a simple transmission line model, and is shown to possess beneficial characteristics. Good coupling is obtained in the practical case where the thickness of the coupling layer is small compared to the acoustic wavelength. Moreover, the silicone produces a highly damped behavior of the transducer, which is necessary in order to achieve good pulse response. These conclusions are verified in the experimental results.

## ACKNOWLEDGEMENTS

This work has been funded by the Commonwealth of Pennsylvania through the Pennsylvania Infrastructure Technology Alliance program, administered at Carnegie Mellon by the Institute for Complex Engineering Systems, and by gifts from Krautkramer Inc., and the authors gratefully acknowledge that support.

## REFERENCES

1. Krautkramer, J. and Krautkramer. H., *Ultrasonic Testing of Materials*, 4<sup>th</sup> edition, Springer Verlag, Berlin, 1989.
2. Ladabaum, I., Jin, X., Soh, H., Atalar, A., and Khuri-Yakub, B., "Surface micromachined capacitive ultrasonic transducers," *IEEE Trans. On Ultrasonics, Ferroelectrics, and Frequency Control*, Vol. 45, 678-690, 1998.



3. Jin, X., Ladabaum, Degertkin, F., Calmes, S., and Khuri-Yakub, B., "Fabrication and characterization of surface micromachined capacitive ultrasonic immersion transducers," *IEEE Jnl. Of Microelectromechanical Systems*, Vol. 8, 100-114, 1999.
4. Hansen, S., Mossawir, B., Ergun, A., Degertkin, F., and Khuri-Yakub, B., "Air-coupled nondestructive evaluation using micromachined ultrasonic transducer," *IEEE Ultrasonics Symposium*, 1037-1040, 1999.
5. Oralkan, O., Jin, X., Kaviani, K., Ergun, A., Degertkin, F., Karaman, M., and Khuri-Yakub, B., "Initial pulse-echo imaging results with one-dimensional capacitive micromachined ultrasonic transducer arrays," *IEEE Ultrasonics Symposium*, 959-962, 2000.
6. Jin, X., Soh, H., Oralkan, O., Degertekin, F., and Khuri-Yakub, B., "Characterization of one-dimensional capacitive micromachined ultrasonic immersion transducer arrays," *IEEE Trans. On Ultrasonics, Ferroelectrics, and Frequency Control*, Vol. 48, 750-760, 2001.
7. Schindel, D., "Air-coupled generation and detection of ultrasonic bulk-waves in metals using micromachined capacitive transducers," *Ultrasonics*, Vol. 35, 179-181, 1995.
8. Bashford, A., Schindel, D., and Hutchins, D., "Micromachined ultrasonic capacitance transducers for immersion applications," *IEEE Trans. On Ultrasonics, Ferroelectrics, and Frequency Control*, Vol. 45, 367-375, 1998.
9. Eccardt, P., Niederer, K., Scheiter, T., and Hierold, C., "Surface micromachined ultrasound transducers in CMOS technology," *IEEE Ultrasonics Symposium*, 959-962, 1996.
10. Eccardt, P., Niederer, K., and Fischer, B., "Micromachined transducers for ultrasound applications," *IEEE Ultrasonics Symposium*, 1609-1618, 1996.
11. Oppenheim, I. J., Jain, A., and Greve, D. W., "A MEMS Ultrasonic Transducer for Resident Monitoring of Steel Structures," SPIE Smart Structures Conference SS05: Systems for Bridges, Structures, and Highways, San Diego, March 2002.
12. Jain, A., Greve, D. W., and Oppenheim, I. J., "A MEMS Phased Array Transducer for Ultrasonic Flaw Detection," IEEE Sensors 2002, Orlando, June 2002.
13. Jain, A., Greve, D. W., and Oppenheim, I. J., "A MEMS Transducer for Ultrasonic Flaw Detection," ISARC 2002, Washington, D.C., September 2002.
14. Greve, D. W., Jain, A., and Oppenheim, I. J., "MEMS Phased Array Detection in Contact with Solids," IEEE Ultrasonics Conference, Munich, October 2002.
15. Greve, D., Oppenheim, I., and Jain, A., "Electrical characterization of coupled and uncoupled MEMS ultrasonic transducers," IEEE Transactions on Ultrasonics, Ferroelectrics, and Frequency Control, scheduled for publication March 2003.
16. Greve, D., Jain, A., and Oppenheim, I., "MEMS ultrasonic transducers for the testing of solids," IEEE Transactions on Ultrasonics, Ferroelectrics, and Frequency Control, scheduled for publication March 2003.